

Neutrinos as Hot or Warm Dark Matter *

Y.F. LI AND ZHI-ZHONG XING

Institute of High Energy Physics and Theoretical Physics Center for Science
Facilities, Chinese Academy of Sciences, Beijing 100049, China

Both active and sterile sub-eV neutrinos can serve for hot dark matter (DM). On the other hand, keV sterile neutrinos could be a good candidate for warm DM. The beta-decaying (e.g., ^3H and ^{106}Ru) and EC-decaying (e.g., ^{163}Ho) nuclei are considered as the most promising targets to capture those extremely low energy neutrinos and antineutrinos, respectively. We calculate the capture rates of relic electron neutrinos and antineutrinos against the corresponding beta-decay or EC-decay backgrounds in different flavor mixing schemes. We stress that such direct laboratory measurements of hot or warm DM might not be hopeless in the long term.

PACS numbers: 13.60.Pq, 13.15.+g, 14.60.St, 95.35.+d

1. Introduction

Although the existence of dark matter (DM) in the Universe has been established, what it is made of remains a fundamental puzzle [1]. Within the standard model (SM) three kinds of active neutrinos and their antiparticles, whose masses lie in the sub-eV range, may constitute hot DM. Beyond the SM one or more species of sterile neutrinos and antineutrinos at a similar mass scale may also form hot DM, if they were thermalized in the early Universe as their active counterparts. Such light sterile particles are hypothetical, but their existence is more or less implied by current experimental and cosmological data. On the one hand, the long-standing LSND antineutrino anomaly [2], the more recent MiniBooNE antineutrino anomaly [3] and the latest reactor antineutrino anomaly [4] can all be interpreted as the active-sterile antineutrino oscillations in the assumption of two kinds of sterile antineutrinos whose masses are close to 1 eV [5]. On the other hand, an analysis of the existing data on the cosmic microwave background

* Presented by Zhi-zhong Xing at the XXXV International Conference of Theoretical Physics — Matter to the Deepest, Ustron, Poland, September 12–18, 2011.

(CMB), galaxy clustering and Type-Ia supernovae favors some extra radiation content in the Universe and one or two species of sterile neutrinos and antineutrinos at the sub-eV mass scale [6]. We are therefore open-minded to conjecture that hot DM might in general consist of both active and sterile components. These relics of the Big Bang form the unseen cosmic neutrino background ($C\nu B$) and cosmic antineutrino background ($C\bar{\nu}B$), whose temperature T_ν is slightly lower than the CMB temperature T_γ (i.e., $T_\nu = \sqrt[3]{4/11} T_\gamma \simeq 1.945$ eV today) [7].

But hot DM only has a tiny contribution to the total matter density of the Universe. A careful analysis of the structure formation indicates that most DM should be cold (nonrelativistic) or warm (semirelativistic) at the onset of the galaxy formation, when the temperature of the Universe was about 1 keV [7]. A number of candidates for cold DM have so far been investigated. In comparison, warm DM is another interesting possibility of accounting for the observed non-luminous and non-baryonic matter content in the Universe. It may allow us to solve or soften several problems that we have recently encountered in the DM simulations [8] (e.g., to damp the inhomogeneities on small scales by reducing the number of dwarf galaxies or to smooth the cusps in the DM halos). A good candidate for warm DM should be sterile neutrinos and antineutrinos, if their masses are in the keV range and their lifetimes are much longer than the age of the Universe [9].

How to detect hot or warm DM neutrinos and antineutrinos is a great challenge to the present experimental techniques. Among several possible ways [10], the most promising one is the relic neutrino capture experiment by means of radioactive beta-decaying nuclei [11]–[18]. The key point is that a generic neutrino capture reaction will take place with no threshold on the incident neutrino energy, provided the mother nuclei can naturally undergo the beta decay with an energy release in the limit of vanishing neutrino masses. The signal of this neutrino capture process is measured by the monoenergetic electron's kinetic energy for each neutrino mass eigenstate, well beyond that of the corresponding beta decay background. A measurement of the gap between the capture and decay processes will directly probe these hot or warm DM neutrinos and determine or constrain their masses and mixing angles. However, this method does not directly apply to the capture of hot or warm DM antineutrinos, simply because it is ν_e (instead of $\bar{\nu}_e$) that is involved in the capture reaction. A possible way out for relic antineutrino detection is to make use of some radioactive nuclei which can decay via electron capture (EC) [19]–[22].

The remaining parts of this talk are organized as follows. In section 2 we summarize the main formulas which can be used to calculate the beta-decay energy spectrum and the relic neutrino capture rate. Section 3 is devoted to the capture of hot or warm DM neutrinos in different flavor

mixing schemes. We shall give a brief description of the relic antineutrino capture on EC-decaying nuclei in section 4, and then conclude in section 5.

2. Relic Neutrino Captures

In the presence of $3 + N_s$ species of active and sterile neutrinos, the flavor eigenstates of three active neutrinos can be written as [1, 7]

$$|\nu_\alpha\rangle = \sum_i V_{\alpha i}^* |\nu_i\rangle, \quad (1)$$

where α runs over e , μ and τ , ν_i is a mass eigenstate of active (for $1 \leq i \leq 3$) or sterile (for $4 \leq i \leq 3 + N_s$) neutrinos, and $V_{\alpha i}$ stands for an element of the $3 \times (3 + N_s)$ neutrino mixing matrix V . For simplicity, we assume that the light sterile neutrinos under consideration do not significantly affect the values of two mass-squared differences and three mixing angles of active neutrinos extracted from current experimental data on solar, atmospheric, reactor and accelerator neutrino oscillations [7]. In this assumption we shall use $\Delta m_{21}^2 \approx 7.6 \times 10^{-5} \text{ eV}^2$ and $|\Delta m_{31}^2| \approx 2.4 \times 10^{-3} \text{ eV}^2$ together with $\theta_{12} \approx 34^\circ$ and $\theta_{13} \approx 10^\circ$ as typical inputs in our numerical estimates. Depending on the sign of Δm_{31}^2 , there are two possible mass patterns for active neutrinos: $m_1 < m_2 < m_3$ (normal hierarchy) or $m_3 < m_1 < m_2$ (inverted hierarchy). In either case the absolute mass scale is unknown, but its upper bound is expected to be of $\mathcal{O}(0.1) \text{ eV}$ as constrained by current cosmological data [23]. We shall specify the values of m_i and $|V_{ei}|$ when calculating the capture rates of relic neutrinos in sections 3.

Let us concentrate on the relic neutrino capture on radioactive beta-decaying nuclei (i.e., $\nu_e + N \rightarrow N' + e^-$). This capture reaction can happen for any kinetic energy of the incident neutrino, because the corresponding beta decay $N \rightarrow N' + e^- + \bar{\nu}_e$ always releases some energies ($Q_\beta = m_N - m_{N'} - m_e > 0$). So it has a unique advantage in detecting cosmic neutrinos with both $m_i \ll Q_\beta$ and extremely low energies [11]–[18]. In the low-energy limit the product of the cross section of non-relativistic neutrinos σ_{ν_i} and the neutrino velocity v_{ν_i} converges to a constant value [13], and thus the differential neutrino capture rate reads

$$\frac{d\lambda_\nu}{dT_e} = \sum_i |V_{ei}|^2 \sigma_{\nu_i} v_{\nu_i} n_{\nu_i} R(T_e, T_e^i), \quad (2)$$

where n_{ν_i} denotes the number density of relic ν_i neutrinos around the Earth. The standard Big Bang model predicts $\langle n_{\nu_i} \rangle \approx \langle n_{\bar{\nu}_i} \rangle \approx 56 \text{ cm}^{-3}$ today for each species of active neutrinos and antineutrinos, and this prediction is also expected to hold for each species of light sterile neutrinos and antineutrinos

if they could be completely thermalized in the early Universe. The number density of hot neutrino and antineutrino DM around the Earth may be more or less enhanced by the gravitational clustering effect when m_i is larger than 0.1 eV [24]. As for the keV sterile neutrinos, we assume their number density could account for the total amount of DM in our Galactic neighborhood. In Eq. (2), $R(T_e, T_e^i)$ is a Gaussian energy resolution function defined by [17]

$$R(T_e, T_e^i) = \frac{1}{\sqrt{2\pi}\sigma} \exp \left[-\frac{(T_e - T_e^i)^2}{2\sigma^2} \right], \quad (3)$$

in which T_e is the overall kinetic energy of the electrons detected in the experiment and $T_e^i = Q_\beta + E_{\nu_i}$ is the kinetic energy of the outgoing electron for each incoming mass eigenstate ν_i . Using Δ to denote the experimental energy resolution, we have $\Delta = 2\sqrt{2\ln 2}\sigma \approx 2.35482\sigma$.

The main background of a neutrino capture process is its corresponding beta decay. The finite energy resolution may push the outgoing electron's ideal endpoint $Q_\beta - \min(m_i)$ towards a higher energy region, and hence it is possible to mimic the desired signal of the neutrino capture reaction. Given the same energy resolution as that in Eq. (2), we can describe the energy spectrum of a beta decay as [25]

$$\begin{aligned} \frac{d\lambda_\beta}{dT_e} &= \int_0^{Q_\beta - \min(m_i)} dT_e' \left\{ \frac{G_F^2 \cos^2 \theta_C}{2\pi^3} F(Z, E_e) |\mathcal{M}|^2 E_e \sqrt{E_e^2 - m_e^2} \right. \\ &\quad \times (Q_\beta - T_e') \sum_{i=1}^4 \left[|V_{ei}|^2 \sqrt{(Q_\beta - T_e')^2 - m_i^2} \Theta(Q_\beta - T_e' - m_i) \right] \Big\} \\ &\quad \times R(T_e, T_e'), \end{aligned} \quad (4)$$

where $T_e' = E_e - m_e$ is the intrinsic kinetic energy of the outgoing electron, $F(Z, E_e)$ denotes the Fermi function, $|\mathcal{M}|^2$ stands for the dimensionless contribution of relevant nuclear matrix elements [25], and $\theta_C \simeq 13^\circ$ is the Cabibbo angle. In Eq. (4) the theta function $\Theta(Q_\beta - T_e' - m_i)$ is adopted to ensure the kinematic requirement. Note that the numerical results of λ_ν and λ_β can be properly normalized by using the half-life of the mother nucleus via the relation ($\lambda_\beta T_{1/2} = \ln 2$). Then the distributions of the numbers of signal and background events are expressed, respectively, as

$$\begin{aligned} \frac{dN_S}{dT} &= \frac{1}{\lambda_\beta} \cdot \frac{d\lambda_\nu}{dT} \cdot \frac{\ln 2}{T_{1/2}} N_T t, \\ \frac{dN_B}{dT} &= \frac{1}{\lambda_\beta} \cdot \frac{d\lambda_\beta}{dT} \cdot \frac{\ln 2}{T_{1/2}} N_T t \end{aligned} \quad (5)$$

for a given target factor N_T (i.e., the number of target atoms) and for a given exposure time t in the experiment.

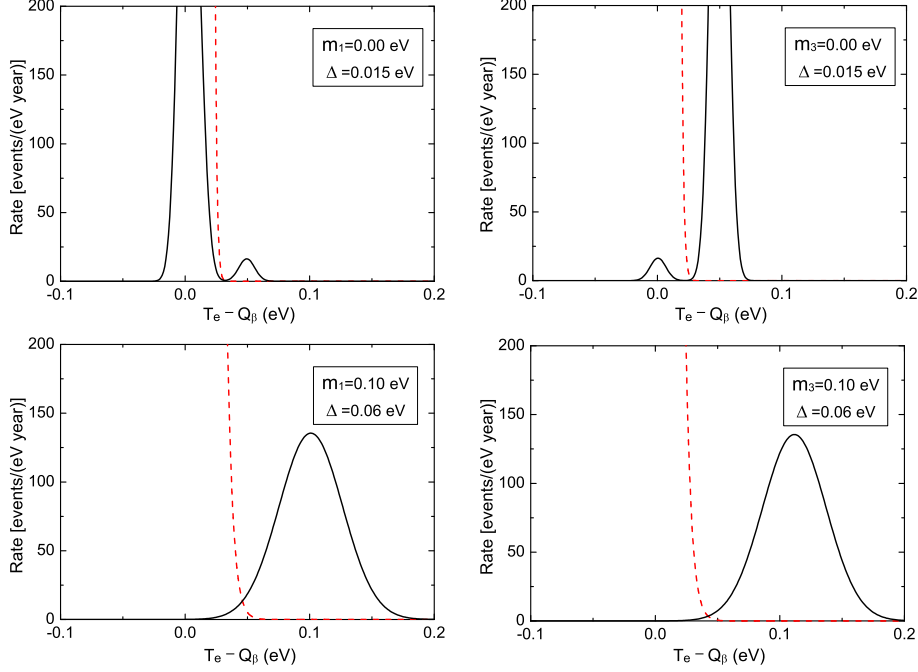


Fig. 1. The relic neutrino capture rate as a function of the kinetic energy of electrons in the standard scheme with $\Delta m_{31}^2 > 0$ (left panel) or $\Delta m_{31}^2 < 0$ (right panel).

3. Hot or Warm DM Neutrinos

We illustrate the relic neutrino capture signals against the beta-decay backgrounds by considering three neutrino mixing schemes: (a) the standard scheme with three sub-eV active neutrinos (hot DM); (b) the (3 + 2) scheme with three sub-eV active neutrinos and two sub-eV sterile neutrinos (hot DM); and (c) the (3 + 1) scheme with three sub-eV active neutrinos and one keV sterile neutrino (warm DM). In our numerical calculations we typically take 100 g ^3H as the radioactive target for the hot DM detection and 10 kg ^3H or 1 ton ^{106}Ru as the isotope source for the warm DM detection.

Fig. 1 shows the relic neutrino capture rate as a function of the kinetic energy T_e of electrons in the standard scheme with $\Delta m_{31}^2 > 0$ in the left panel and $\Delta m_{31}^2 < 0$ in the right panel. The finite energy resolution Δ is taken in such a way that only one single peak can be observed beyond the background. To illustrate the flavor effects, we fix two mass-squared differences and three mixing angles with the typical values given in section 2. Eq. (2) tells us that the contribution of each neutrino mass eigenstate ν_i (for $i = 1, 2, 3$) to the capture rate is located at $T_e^i = Q_\beta + E_{\nu_i}$ and weighted by the relic neutrino number density (we assume $n_{\nu_i} = \langle n_{\nu_i} \rangle \simeq 56 \text{ cm}^{-3}$) and

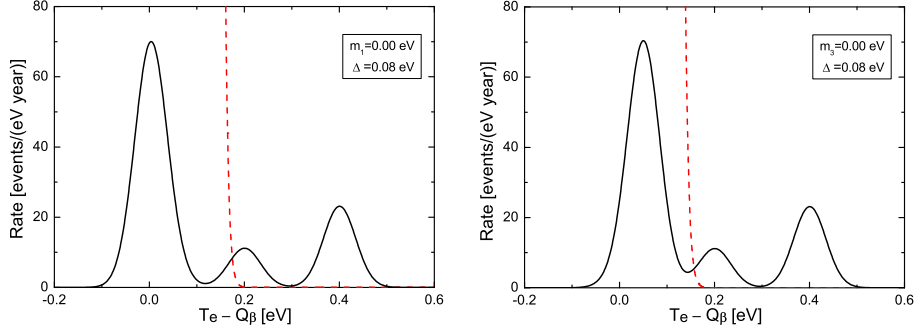


Fig. 2. The relic neutrino capture rate as a function of the kinetic energy of electrons in the $(3 + 2)$ scheme with $\Delta m_{31}^2 > 0$ (left panel) and $\Delta m_{31}^2 < 0$ (right panel). The gravitational clustering of relic sterile neutrinos around the Earth has been illustrated by taking $\zeta_1 = \zeta_2 = \zeta_3 = 1$ and $\zeta_5 = 2\zeta_4 = 10$ for example.

the flavor mixing matrix element $|V_{ei}|^2$. On the other hand, Eq. (4) tells us that the energy spectrum of the beta decay near its endpoint is dominated by the lightest neutrino mass eigenstate hidden in ν_e and sensitive to the energy resolution Δ . As the smallest neutrino mass (m_1 in the left panel of Fig. 1 or m_3 in the right panel of Fig. 1) increases from 0 to 0.1 eV, the capture signal moves towards the larger $T_e - Q_\beta$ region. In comparison, the shift of the corresponding background is less obvious because the smallest neutrino mass and Δ have the opposite effects on the location of the spectral endpoint of the beta decay. Hence the distance between the peak of the signal and the background becomes larger for a larger value of the smallest neutrino mass, and accordingly the required energy resolution Δ becomes less stringent. Comparing between the left and right panels, one can also see that it is more or less easier to detect relic neutrinos in the $\Delta m_{31}^2 < 0$ case, where the signal is separated more obviously from the background. The reason is simply that the dominant neutrino mass eigenstates ν_1 and ν_2 have slightly larger eigenvalues in this case than in the $\Delta m_{31}^2 > 0$ case.

Now we look at the $(3 + 2)$ scheme with two sub-eV sterile neutrinos. Considering the preliminary hints of sub-eV sterile neutrinos [5, 6], we simply assume $m_4 = 0.2$ eV and $m_5 = 0.4$ eV together with $|V_{e1}| \approx 0.792$, $|V_{e2}| \approx 0.534$, $|V_{e3}| \approx 0.168$, $|V_{e4}| \approx 0.171$ and $|V_{e5}| \approx 0.174$ in our numerical estimates. With the help of Eqs. (2) and (3), we are able to calculate the relic neutrino capture rate as a function of the kinetic energy T_e of electrons against the corresponding background for both $\Delta m_{31}^2 > 0$ and $\Delta m_{31}^2 < 0$ cases in Fig 2. We have taken $m_1 = 0$ or $m_3 = 0$ for simplicity. To illustrate possible gravitational clustering effects, we typically take $\zeta_1 = \zeta_2 = \zeta_3 = 1$ (without clustering effects for three active neutrinos because their maximal

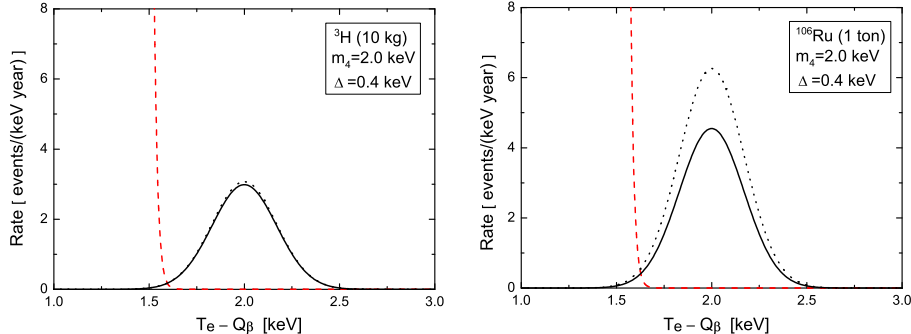


Fig. 3. The keV sterile neutrino capture rate as a function of the kinetic energy of electrons with ${}^3\text{H}$ (left panel) and ${}^{106}\text{Ru}$ (right panel) as our target sources. The solid (or dotted) curves denote the signals with (or without) the half-life effect.

mass is about 0.05 eV in the scenario under discussion) and $\zeta_5 = 2\zeta_4 = 10$ (with mild clustering effects for two sterile neutrinos because their masses are 0.2 eV and 0.4 eV, respectively). As shown in Fig. 2, the signals of two sterile neutrinos are obviously enhanced due to $\zeta_4 > 1$ and $\zeta_5 > 1$. If the gravitational clustering of non-relativistic neutrinos is very significant around the Earth, it will be very helpful for us to detect the relic neutrinos by means of the neutrino capture processes.

Next let us discuss the detection prospects of keV warm DM neutrinos. In the $(3 + 1)$ scheme the mass and mixing element of the keV sterile neutrino are strictly constrained by current observational data [9]. Here we take $m_4 = 2$ keV and $|V_{e4}|^2 \simeq 5 \times 10^{-7}$ for illustration, and assume $\Delta m_{31}^2 > 0$ and $m_1 = 0$. Our results are given in Fig. 3, where two different isotope sources (i.e., 10 kg ${}^3\text{H}$ and 1 ton ${}^{106}\text{Ru}$) are considered to make a comparison. We see that it is easy to achieve the required energy resolution. The main problem which makes the observability rather dim and remote is the extremely small active-sterile neutrino mixing angle. We display the half-life effects for both isotopes in Fig. 3. The finite lifetime is important for the source of ${}^{106}\text{Ru}$ nuclei but negligible for that of ${}^3\text{H}$ nuclei. It may reduce about 30% of the neutrino capture rate on ${}^{106}\text{Ru}$ in the vicinity of $T_e - Q_\beta \simeq m_4$. Hence this effect must be taken into account if the duration of such an experiment is comparable with the half-life of the source.

4. Hot or Warm DM Antineutrinos

As mentioned in section 1, the beta-decaying nuclei can only be used as the targets of relic neutrino captures and one should employ the EC-decaying nuclei to detect relic antineutrinos. In this section we just give a

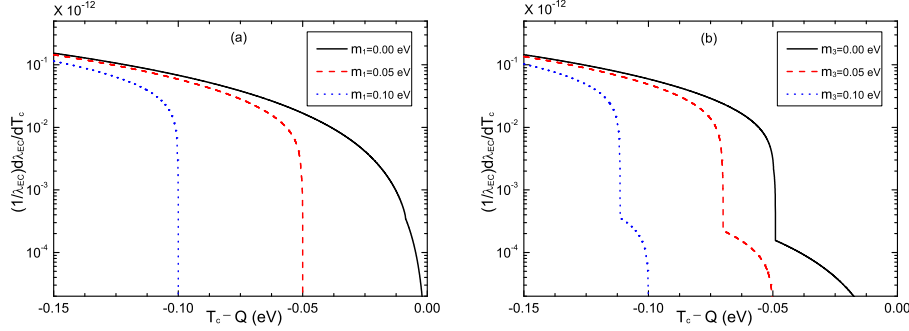


Fig. 4. The fine structure spectrum near the endpoint of the ^{163}Ho EC decay in the $m_{31}^2 > 0$ (left panel) or $m_{31}^2 < 0$ (right panel) case.

brief discussion about the feasibility of this method by considering the rather stable isotope ^{163}Ho [20] as our target. We want to emphasize that the fine structure near the spectral endpoint of the ^{163}Ho EC decay could be used to study the lepton flavor effects in a similar manner as that of beta decays. Comparing between the left and right panels of Fig. 4 might allow one to distinguish between the normal and inverted neutrino mass hierarchies. The properties of the antineutrino capture rate against its background are more or less the same as those discussed in section 3. The detection method can in principle be applied to hot DM (sub-eV active and sterile antineutrinos) and even warm DM (keV sterile antineutrinos). We show two numerical examples in Fig. 5 for illustration. The standard scheme with $\Delta m_{31}^2 > 0$ and $m_1 = 0.1$ eV is depicted in the left panel and a total rate of one event per year needs 30 kg ^{163}Ho . In the right panel we assume the existence of a keV sterile antineutrino with the same mass and mixing angle as the keV sterile neutrino discussed in section 3. It turns out that we need as much as 600 ton ^{163}Ho to get one event per year. So it is almost hopeless in this scenario. Much more discussions can be found in our recent works [21, 22].

5. Concluding Remarks

To pin down what DM is really made of has been one of the most important and most challenging problems in particle physics and cosmology. Both the active and sterile species of sub-eV neutrinos and antineutrinos might be a part of hot DM, and keV sterile neutrinos and antineutrinos could be a good candidate for warm DM. Here we have addressed ourselves to the direct laboratory detection of possible contributions of relic neutrinos and antineutrinos to DM. The beta-decaying (e.g., ^3H and ^{106}Ru) and EC-

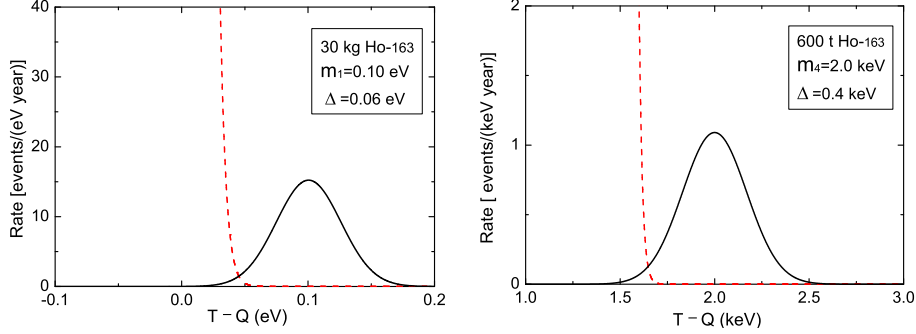


Fig. 5. The antineutrino capture rate as a function of the overall energy release for hot DM antineutrinos (left panel) and warm DM antineutrinos (right panel).

decaying (e.g., ^{163}Ho) nuclei have been considered as the most promising targets to capture such low-energy neutrinos and antineutrinos, respectively. Our analysis shows that the signatures of hot or warm DM neutrinos and antineutrinos should in principle be observable, provided the target is big enough, the energy resolution is good enough and the gravitational clustering effect is significant enough. We admit that our numerical results are quite preliminary and mainly serve for illustration, but we stress that such a direct laboratory search for hot or warm DM neutrinos and antineutrinos is fundamentally important and deserves further attention and more detailed investigations. Although the present experimental techniques are unable to lead us to a guaranteed measurement of relic neutrinos and antineutrinos in the near future, we might have a chance to make a success of this great exploration in the long term.

6. Acknowledgements

One of us (Z.Z.X.) would like to thank M. Biesiada for his kind invitation and warm hospitality in Ustron, where this wonderful conference was held. This work was supported in part by the China Postdoctoral Science Foundation under grant No. 20100480025 (Y.F.L.) and in part by the National Natural Science Foundation of China under grant No. 10875131 (Z.Z.X.).

REFERENCES

- [1] See, e.g., Z.Z. Xing and S. Zhou, *Neutrinos in Particle Physics, Astronomy and Cosmology* (Zhejiang University Press and Springer-Verlag, 2011).
- [2] A. Aguilar *et al.* (LSND Collaboration), Phys. Rev. D **64**, 112007 (2001).

- [3] A.A. Aguilar-Arevalo *et al.* (MiniBooNE Collaboration), Phys. Rev. Lett. **105**, 181801 (2010).
- [4] G. Mention *et al.*, Phys. Rev. D **83**, 073006 (2011).
- [5] J. Kopp, M. Maltoni, and T. Schwetz, Phys. Rev. Lett. **107** 091801 (2011).
- [6] J. Hamann *et al.*, Phys. Rev. Lett. **105**, 181301 (2010).
- [7] Particle Data Group, K. Nakamura *et al.*, J. Phys. G **37**, 075021 (2010).
- [8] P. Bode, J.P. Ostriker, and N. Turok, Astrophys. J. **556**, 93 (2001).
- [9] A. Kusenko, Phys. Rept. **481**, 1 (2009).
- [10] A. Ringwald, Nucl. Phys. A **827**, 501c (2009).
- [11] S. Weinberg, Phys. Rev. **128**, 1457 (1962).
- [12] J.M. Irvine and R. Humphreys, J. Phys. G **9**, 847 (1983).
- [13] A. Cocco, G. Mangano, and M. Messina, JCAP **0706**, 015 (2007).
- [14] R. Lazauskas, P. Vogel, and C. Volpe, J. Phys. G **35**, 025001 (2008).
- [15] M. Blennow, Phys. Rev. D **77**, 113014 (2008).
- [16] Y.F. Li and Z.Z. Xing, Phys. Lett. B **695**, 205 (2011).
- [17] Y.F. Li, Z.Z. Xing, and S. Luo, Phys. Lett. B **692**, 261 (2010).
- [18] H.J. de Vega *et al.*, arXiv:1109.3452 [hep-ph].
- [19] A.G. Cocco, G. Mangano, and M. Messina, Phys. Rev. D **79**, 053009 (2009).
- [20] M. Lusignoli and M. Vignati, Phys. Lett. B **697**, 11 (2011).
- [21] Y.F. Li and Z.Z. Xing, Phys. Lett. B **698**, 430 (2011).
- [22] Y.F. Li and Z.Z. Xing, JCAP **1108**, 006 (2011).
- [23] E. Komatsu *et al.* (WMAP Collaboration), Astrophys. J. Supp. **192**, 18 (2011).
- [24] A. Ringwald and Y.Y.Y. Wong, JCAP **0412**, 005 (2004).
- [25] E.W. Otten and C. Weinheimer, Rept. Prog. Phys. **71**, 086201 (2008).